CHIN. PHYS. LETT. Vol. 29, No. 10 (2012) 108502

Photo-Induced Spin Dynamics in Nanoelectronic Devices

Mina D. Asham[1**], Walid A. Zein[2], Adel H. Phillips[2**]
[1]*Faculty of Engineering, Benha University, Benha, Egypt*
[2]*Faculty of Engineering, Ain-Shams University, Cairo, Egypt*

(Received 20 February 2012)

The present research is devoted to the investigation of electron spin transmission through a nanoelectronic device. This device is modeled as nonmagnetic semiconductor quantum dot coupled to two diluted magnetic semiconductor leads. The spin transport characteristics through such a device are investigated under the effect of an ac-field of a wide range of frequencies. The present result shows a periodic oscillation of the conductance for both the cases of parallel and antiparallel spin alignment. These oscillations are due to Fano-resonance. Results for spin polarization and giant magneto-resistance show the coherency property. The present research might be useful for developing single spin-based quantum bits (qubits) required for quantum information processing and quantum spin-telecommunication.

PACS: 85.75.−d, 85.75.Hh, 85.35.Be DOI: 10.1088/0256-307X/29/10/108502

Control of spin-polarized electric conduction while maintaining phase coherence is needed for quantum information technology.[1,2] Spintronics is based on three factors: spin injection, control of spin transport, and spin selective detection.[1−5]

In recent years, spin polarized transport through II–VI diluted magnetic semiconductors/nonmagnetic semiconductor junctions has attracted much attention due to its potential use in spintronics.[6−8] Diluted magnetic semiconductors of II–VI compounds have attracted a considerable attention for the last few years due to the carrier-mediated origin of the ferromagnetism.[9] This special feature makes it possible to control quantization of the material by changing the concentration of the carriers, which is required property for future applications in semiconductor spintronics and in optoelectronic devices.[9,10] The II–VI diluted magnetic semiconductors are known to be good candidates for effective spin injection into a nonmagnetic semiconductor because their spin polarization can be easily detected.[11,12]

Quantum dots are semiconductor heterostructures in which carriers are confined in all three space dimensions.[13,14] Their discrete energy spectrum, tunable in a wide range by structural design, in combination with the ability to embed quantum dots in a practical device environment, predestines these nanostructures for various applications in optoelectronics, spintronics, and quantum information processing.[2,3] Electron spin qubits are based on Zeeman-state doublets, coupled by microwave irradiation at the resonance frequency. The microwave irradiation drives spin resonance and manipulation with pulses of appropriate duration.[15] It may also activate electron spin transport in the quantum dot via inelastic tunneling due to exchanges of energy between electron spins and the microwave field (photon-assisted tunneling, PAT).[16−19]

In this Letter, we investigate the spin transport characteristics through a nanoelectronic device under the effect of both ac-field (mid-infrared) of different frequencies and magnetic field. The investigated nanoelectronic device consists of a semiconducting quantum dot coupled to two diluted magnetic semiconductor leads. The spin-transport of electrons through such a device is conducted under the effect of both ac-field (mid-infrared) of a wide range of frequencies and magnetic effect (see Fig. 1). The oscillating ac-field introduces additional photon-assisted conduction channels that can be tuned via a gate voltage to lie within the conduction window of the device. In the presence of Zeeman splitting produced by an applied magnetic field, the contribution from the photon-assisted channels becomes different for spin up and spin down resulting in photon-assisted spin polarized conductance.

Thus, it is desirable to deduce an expression for spin-polarization and giant magneto-resistance. This is carried out as follows: the Hamiltonian H describing the spin transport of electrons through such a nanodevice can be written as

$$H = -\frac{\hbar^2}{2m^*}\frac{d^2}{dx^2} + eV_{\rm sd} + eV_{\rm g} + E_{\rm F} + V_{\rm b} + eV_{\rm ac}\cos(\omega t) \pm \frac{1}{2}g\mu_{\rm B}\sigma B + \frac{N^2e^2}{2C} \pm \sigma h_{\rm o}, \quad (1)$$

where m^* is the effective electron mass, h is the reduced Planck constant, $V_{\rm sd}$ is the source-drain voltage (bias voltage), $V_{\rm g}$ is the gate voltage, $E_{\rm F}$ is the Fermi-energy, $V_{\rm b}$ is the barrier height at the interface between the leads and the quantum dot, $V_{\rm ac}$ is the amplitude of the applied ac-field with frequency ω, g is the Landé factor of the diluted magnetic semiconductor, $\mu_{\rm B}$ is Bohr magneton, B is the applied magnetic field, σ represents the Pauli matrices of spin, and $h_{\rm o}$ is the exchange field of the diluted magnetic semiconductor. In Eq. (1), the term $N^2e^2/2C$ represents the Coulomb charging energy of the quantum

**Corresponding author. Email: adel.phillips@gmail.com; minadanial@yahoo.com
© 2012 Chinese Physical Society and IOP Publishing Ltd

dot in which e is the electron charge, N is the number of electrons tunneling through the quantum dot, and C is the capacitance of the quantum dot. Therefore, the corresponding Schrödinger equation for such transport reads

$$H\psi = E\psi, \tag{2}$$

where the solution for the eigenfunction, $\psi(x)$, in the corresponding regions of the device, can be expressed as[20]

$$\psi(x) = \begin{cases} \sum_{n=1}^{\infty} [A_1 e^{ik_1 x} + B_1 e^{-ik_1 x}] J_n\left(\frac{eV_{\rm ac}}{\hbar\omega}\right) e^{-in\omega t}, & x < 0 \\ \sum_{n=1}^{\infty} [A_2 Ai(\rho(x)) + B_2 Bi(\rho(x))] J_n(\frac{eV_{\rm ac}}{\hbar\omega}) e^{-in\omega t}, & 0 < x < d \\ \sum_{n=1}^{\infty} A_3 e^{ik_2 x} J_n(\frac{eV_{\rm ac}}{\hbar\omega}) e^{-in\omega t}, & x > d \end{cases} \tag{3}$$

where $Ai(\rho(x))$ is the Airy function and its complement is $Bi(\rho(x))$.[21] In Eqs. (3), the parameter $J_n\,(eV_{\rm ac}/h\omega)$ represents the $n^{\rm th}$ order Bessel function of the first kind. The solutions to Eqs. (3) must be generated by the presence of the different side-bands n which come with phase factor $e^{-in\omega t}$,[16–19] and d represents the diameter of the quantum dot. Also, the parameters k_1, k_2 and $\rho(x)$ in Eqs. (3) can be expressed as

$$k_1 = \sqrt{\frac{2m^*}{\hbar^2}(E + n\hbar\omega + V_{\rm b} + \sigma h_{\rm o})}, \quad n = 0, \pm 1, \pm 2, \pm 3, \ldots \tag{4}$$

$$k_2 = \left[\frac{2m^*}{\hbar^2}\left(V_{\rm b} + eV_{\rm sd} + eV_{\rm g} + E_{\rm F} + \frac{N^2e^2}{2C} + n\hbar\omega \pm \frac{1}{2}g\mu_{\rm B}B\sigma \pm \sigma h_{\rm o}\right)\right]^{1/2}, \tag{5}$$

$$\rho(x) = \frac{d}{eV_{\rm sd}\,\Phi}\left[E_{\rm F} + V_{\rm b} + eV_{\rm sd}\left(\frac{x}{d}\right) + eV_{\rm g} + \frac{N^2e^2}{2C} + \frac{1}{2}g\mu_{\rm B}B\sigma + E\right], \tag{6}$$

where Φ is given by

$$\Phi = \sqrt[3]{\frac{\hbar^2 d}{2m^* eV_{\rm sd}}}. \tag{7}$$

Now, the tunneling probability $\Gamma(E)$ can be obtained by applying the boundary conditions to the eigenfunctions (Eqs. (3)) and their derivatives at the boundaries of the junction.[16–19] We obtain the following expression for the tunneling probability,

$$\Gamma(E) = \sum_{n=1}^{\infty} J_n^2\left(\frac{eV_{\rm ac}}{\hbar\omega}\right) \cdot \left\{\frac{4k_1k_2}{\pi^2\Phi^2}[\alpha^2k_1^2k_2^2 + \beta^2 m^{*^2}k_1^2]^{-1}\right\}, \tag{8}$$

where α and β are given by

$$\alpha = Ai(\rho(0)) \cdot Bi(\rho(d)) - Bi(\rho(0)) \cdot Ai(\rho(d)), \tag{9}$$

$$\beta = \frac{1}{\Phi m^*}[Ai(\rho(0)) \cdot Bi'(\rho(d)) - Bi(\rho(0)) \cdot Ai'(\rho(d))]. \tag{10}$$

Here $Ai'(\rho(x))$ is the first derivative of the Airy function and $Bi'(\rho(x))$ is the first derivative of its complement.

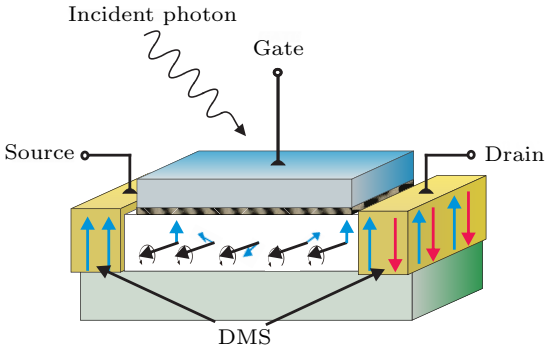


Fig. 1. Schematics of a spin transistor. Spin polarized electrons (blue arrows) are injected from a DMS source contact into a semiconductor channel where the spin orientation is controlled by the electric field of a non-magnetic gate contact and analyzed by a DMS drain contact. The black arrows schematically depict the effective magnetic field that results from the electric gate field and the wave vector of the electrons. The blue and red arrows in the drain contact depict the parallel and antiparallel spin alignment, respectively.

Now, the conductance G of the present nanodevice is expressed in terms of the tunneling probability $\Gamma(E)$ through the following Landuaer–Buttiker equation[16–19,22]

$$G = \frac{2e^2}{h}\sin(\varphi)\int_{E_{\rm F}}^{E_{\rm F}+n\hbar\omega} dE\left(-\frac{\partial f_{\rm FD}}{\partial E}\right) \cdot \Gamma(E), \tag{11}$$

where ϕ is the phase of the scattered electrons and $(-\partial f_{\rm FD}/\partial E)$ is the first derivative of the Fermi–Dirac distribution function given by

$$\left(-\frac{\partial f_{\rm FD}}{\partial E}\right) = (4k_{\rm B}T)^{-1}\cosh^{-2}\left(\frac{E - E_{\rm F} + n\hbar\omega}{2k_{\rm B}T}\right), \tag{12}$$

where $k_{\rm B}$ is the Boltzmann constant and T is the absolute temperature.

The spin polarization (SP) and the giant magnetoresistance (GMR) are expressed in terms of the conductance G as follows:[23]

$$\text{SP} = \frac{G_{\uparrow\uparrow} - G_{\uparrow\downarrow}}{G_{\uparrow\uparrow} + G_{\uparrow\downarrow}}, \tag{13}$$

$$\text{GMR} = \frac{G_{\uparrow\uparrow} - G_{\uparrow\downarrow}}{G_{\uparrow\uparrow}}, \tag{14}$$

where $G_{\uparrow\uparrow}$ is the conductance when the magnetization of the two diluted magnetic-semiconductor leads are in parallel alignments, while $G_{\uparrow\downarrow}$ is the conductance

for the case of antiparallel alignment of the magnetization in the leads. The indicator ↑ corresponds to spin up and ↓ corresponds to spin down.

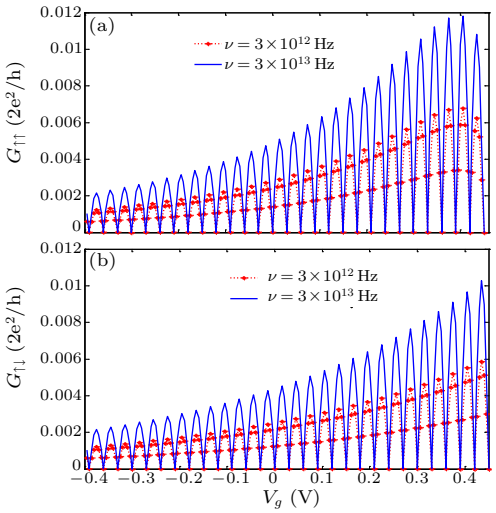


Fig. 2. The variation of conductance with gate voltage at two different frequencies for (a) parallel spin alignment and (b) antiparallel spin alignment.

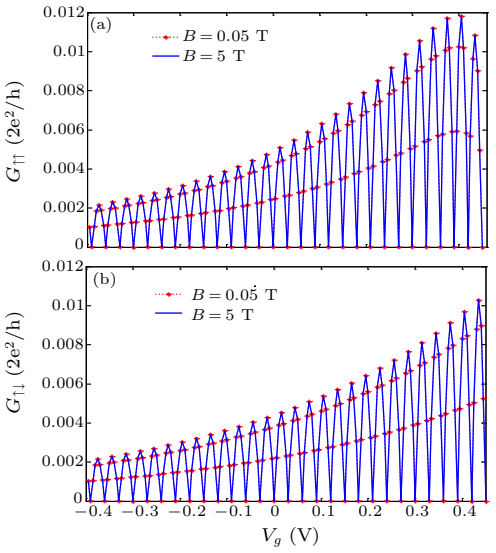


Fig. 3. The variation of conductance with gate voltage at two different values of magnetic field for (a) parallel spin alignment and (b) antiparallel spin alignment.

It is interesting to calculate the cutoff frequency $\nu_{\rm T}$ of the nanoelectronic device studied here, which is expressed in terms of the maximum conductance $G_{\max}$ for both parallel and antiparallel alignment spins via the following equation:[20]

$$\nu_{\rm T} = \frac{G_{\max(\uparrow\uparrow/\uparrow\downarrow)}}{2\pi C}, \tag{15}$$

where C is the gate-to-semiconducting-quantum-dot capacitance.

Numerical calculations are performed of Eqs. (11) and (13)–(15), taking into consideration of the two cases for parallel and antiparallel spins of quasiparticles in the two leads. In the present calculations, we take the case of a GaAs quantum dot and the two leads as diluted magnetic semiconductors of GaMnAs. The values for the quantum dot are[16–19,24–26] $E_{\rm F} = 0.75\,{\rm eV}$, $C = 10^{-16}\,{\rm F}$ and $d = 2\,{\rm nm}$, $V_{\rm b} = 0.3\,{\rm eV}$. The value of the exchange field $h_{\rm o}$ for GaMnAs is $-1\,{\rm eV}$ and $g = 2$.[23,27]

The features of the present results are described in the following.

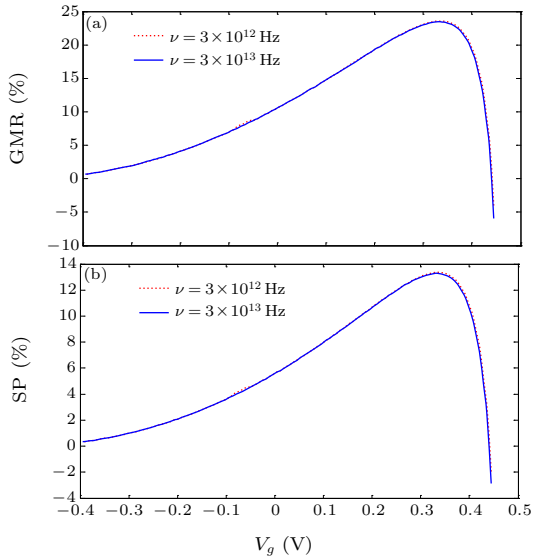


Fig. 4. The variation of (a) GMR and (b) SP with gate voltage at two different frequencies.

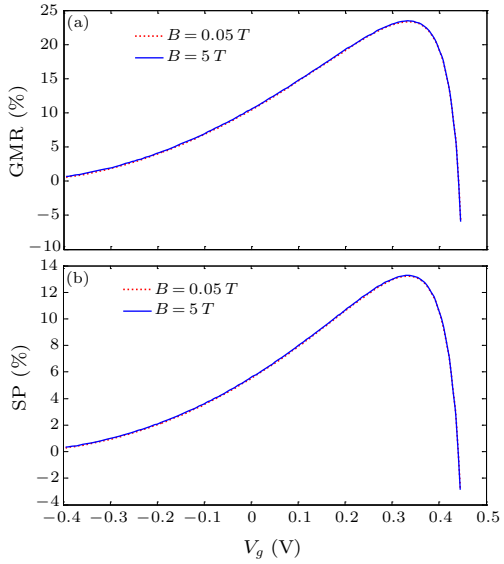


Fig. 5. The variation of (a) GMR and (b) SP with gate voltage at two different values of magnetic field.

The variations of conductance with gate voltage at different frequencies of the ac-field and different magnetic field are shown in Figs. 2(a), 2(b), 3(a), 3(b). The frequencies of the induced ac-field are the frequencies of mid-infrared radiation.

The conductance is calculated for both parallel and antiparallel alignment of spin in the two diluted magnetic semiconductor leads. As shown from the figures,

a periodic oscillation of the conductance for both the cases of alignment, i.e., for $G_{\uparrow\uparrow}$ and $G_{\uparrow\downarrow}$, is observed. Also, we notice that the peak height of conductance ($G_{\uparrow\uparrow}$, $G_{\uparrow\downarrow}$) increases as the gate voltage increases and the width of the half maximum is approximately constant. Spin transport through a semiconducting quantum dot at low temperature reveals new effects such as spin single electron tunneling according to the present results and according to the results obtained by other authors.[28–31] The most important property of this spin single-electron transport is that the conductance for both the cases of spin parallel and antiparallel alignment is a periodic function of the gate voltage (see Figs. 2(a), 2(b), 3(a), 3(b)).

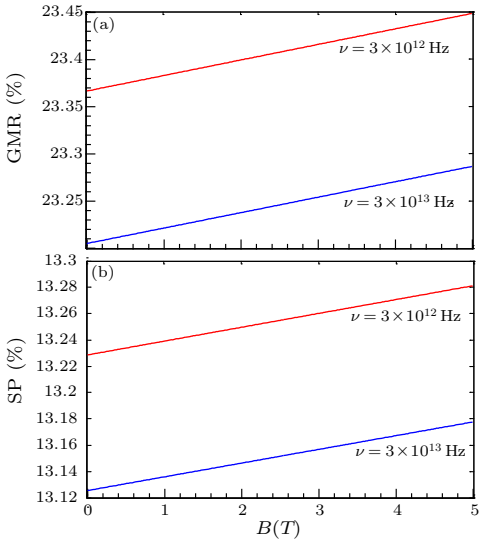


Fig. 6. The variation of (a) GMR and (b) SP with the magnetic field at two different values of frequencies.

According to the present nanoelectronic device model, the interaction of electrons of both spin up and spin down with the induced ac-field (mid-infrared radiation) leads to photon-mediated transmission resonances. The interplay between the induced photons and the spin-up and spin-down electrons leads to so-called Fano-resonance.[19,32–34]

Now, the SP (Eq. (13)) and GMR (Eq. (14)) are calculated. The variations of both spin polarization and giant magneto-resistance with the gate voltage at different frequencies of the induced ac-field (mid-infrared radiation) and at different magnetic field are shown in Figs. 4(a), 4(b), 5(a), 5(b). As shown in these figures, the values of both spin polarization and giant magneto-resistance coincide when the values of both frequencies of induced mid-infrared radiation and applied magnetic field vary. Also, we notice that the trends of the figures are similar and the giant magneto-resistance attains a maximum value approximately ∼23.44% at $V_g \approx 0.335$ V for both the cases (see Figs. 4(a) and 5(a)). The spin polarization attains a maximum value ∼13.28% at $V_g \approx 0.335$ V (see Figs. 4(b) and 5(b)). These results show that the coherent manipulation of the precession of spin polarization could be achieved by the parameters investigated here. This coherency in spin transport through such a nanoelectronic device is a fundamental issue in view of developing single spin-based quantum bits (qubits).[35–38]

In order to confirm the results shown in Figs. 4(a), 4(b), 5(a), 5(b), calculations of giant magneto-resistance and spin polarization with the dependence on the magnetic field are performed. Thus, Figs. 6(a) and 6(b) show the variation of both giant magneto-resistance and spin polarization with the magnetic field at two different frequencies of the induced mid-infrared radiation. These variations are linear for both parameters (see Figs. 6(a) and 6(b)). We notice that the difference between the maximum value of the giant magneto-resistance and its minimum value is approximately 0.08% for both the values of frequencies. Also, the difference between the maximum value of the spin polarization and its minimum value is approximately 0.05% for both the values of frequencies. These results may indicate that the presently proposed nanoelectronic device is stable under the effect of the magnetic field, which is needed in data storage and quantum information processing.[35–38]

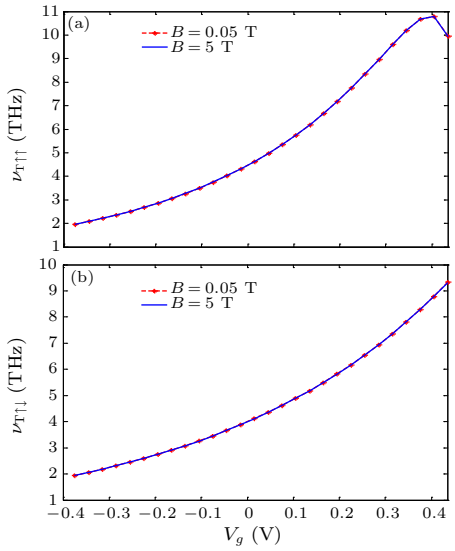


Fig. 7. The variation of the cutoff frequency with gate voltage at two different values of magnetic field for (a) parallel spin alignment and (b) antiparallel spin alignment.

Figures 7(a) and 7(b) show the variations of the cutoff frequency with the gate voltage at two different values of magnetic field for parallel and antiparallel spin alignments, respectively. It is clear that the curves representing different values of magnetic field coincide, emphasizing the weak influence of the magnetic field due to single-electron tunneling. The tunability of the cutoff frequency with the gate voltage is noticed as the value of the cutoff frequency increases with the gate voltage for both the cases of alignment. For the case of parallel spin alignment, the curve reaches a maximum of $\sim 10.8 \times 10^{12}$ Hz at $V_g \sim 0.4$ V. These results have a great impact on the

applications of recent nanodevices and their response to the working frequencies.

We can conclude that the present investigation may be useful for devising the present nanodevice with controllable parameters, for example, the frequency of the induced photons and magnetic field. The presently proposed nanodevice can be manufactured, and can be used in data storage and nonvolatile magnetic memory devices.[10] Also, this nanodevice can be used as a photodetector for a specific frequency of a certain ac-field.[33]

References

[1] Daughton J M, Pohm A V, Fayfield R T and Smith C H 1999 *J. Phys. D: Appl. Phys.* **32** 22 R169
[2] Fabian J, Matos-Abiaguea A, Ertlea C, Stano P and Zutic I 2007 *Acta Phys. Slovaca* **57** 565
[3] Žutić I, Fabian J and Das Sarma S 2004 *Rev. Mod. Phys.* **76** 323
[4] Rashaba E I 2004 *Physica* E **20** 189
[5] Awschalom D D and Flatte M E 2007 *Nat. Phys.* **3** 153
[6] Zhu Z G and Su G 2004 *Phys. Rev.* B **70** 193310
[7] Papp G, Borza S and Peeters F M 2006 *Phys. Status Solidi* B **243** 1956
[8] Vali R and Mirzanian S M 2009 *Solid State Commun.* **149** 2032
[9] Dietl T 1994 *Diluted Magnetic Semiconductors* in *Handbook of Semiconductors* ed Moharjan S (Amesterdam: North-Holland) 3B
[10] Meilikhov E Z and Farzetdinova R M 2010 *J. Exp. Theor. Phys.* **110** 794
[11] Bejar M, Sanchez D, Platero G and McDonald A H 2003 *Phys. Rev.* B **67** 045324
[12] Guo Y, Han L, Zhu R and Xu W 2008 *Eur. Phys. J.* B **62** 1 45
[13] Beenakker C W J 1991 *Phys. Rev.* B **44** 1646
[14] Loss D and DiVincenzo D P 1998 *Phys. Rev.* A **57** 120
[15] Koppens F H L, Buizert C, Tielrooji K J, Vink I T, Nowack K C, Meunier T, Kowenhoven L P and Vandersypen L M K 2006 *Nature* **442** 766
[16] Amin A F, Li G Q, Phillips A H and Kleinekathofer U 2009 *Eur. Phys. J.* B **68** 103
[17] Zein W A, Ibrahim N A and Phillips A H 2010 *Prog. Phys.* **4** 78
[18] Zein W A, Ibrahim N A and Phillips A H 2011 *Prog. Phys.* **1** 65
[19] Zein W A, Ibrahim N A and Phillips A H 2011 *Phys. Res. Int.* **2011** 505091
[20] Manasreh O 2005 Semiconductor Heterojunctions and Nanostructures (New York: McGraw-Hill)
[21] Abramowitz M and Stegun I A 1965 *Handbook of Mathematical Functions* (New York: Dover)
[22] Heinzel T 2003 *Mesoscopic Electronics in Solid State Nanostructures* (New York: Wiley-VCH)
[23] Maekawa S and Shinjo T 2002 *Spin-dependent Transport in Magnetic Nanostructures* (Florida: CRC Press)
[24] Aly A H and Phillips A H 2002 *Phys. Status Solidi* B **232** 283
[25] Aly A H, Hong J and Phillips A H 2006 *Int. J. Mod. Phys.* B **20** 2305
[26] Phillips A H, Mina A N, Sobhy M S and Fouad E A 2007 *J. Comput. Theor. Nanosci.* **4** 174
[27] Sanvito S, Theurich G and Hill N 2002 *J. Supercond. Novel Magn.* **15** 85
[28] Attallah A S, Phillips A H, Amin A F and Semary M A 2006 *Nano* **1** 259
[29] Phillips A H, Aly N A I, Kirah K and El-Sayes H E 2008 *Chin. Phys. Lett.* **25** 250
[30] Bernas J and Weymann I 2008 *J. Phys.: Condens. Matter* **20** 423202
[31] Zutic I, Fabian J and Ertler C 2011 *Comprehensive Semicond. Sci. Technol.* **6** 615
[32] Miroshnickenko A E, Flash S and Kivshar Y S 2010 *Rev. Mod. Phys.* **82** 2257
[33] Zhang C X, Nie Y H and Liang J Q 2006 *Phys. Rev.* B **73** 085307
[34] Perfetto E, Stefanucci G and Cini M 2008 *Phys. Rev.* B **78** 155301
[35] John Peter A and Lily Mary Eucharista K 2009 *J. Magn. Magn. Mater.* **321** 402
[36] Vrijen R and Yablonovitch E 2001 *Physica* E **10** 569
[37] Trocha P 2010 *Phys. Rev.* B **82** 115320
[38] Souza F M, Carrara T L and Veruek E 2011 *Phys. Rev.* B **84** 115322